

Estimating and validating basin-scale actual evapotranspiration using MODIS images and hydrologic models

Xiuqin Fang, Liliang Ren, Qiongfang Li, Xiaofan Liu, Fei Yuan, Dengzhong Zhao and Qian Zhu

ABSTRACT

An algorithm for estimating daily spatial actual evapotranspiration (ET) from remotely sensed MODIS data is presented. It is based on the surface energy balance scheme and the modified Priestley–Taylor equation, and has been applied to the MODIS data acquired during growing seasons over the Laohahe River basin, northeastern China. Spatial distributed mapping of daily ET for 22 clear sky days in the year of 2000 from MODIS images over the study area were obtained. In order to validate ET values estimated from MODIS data, regional daily ET values were calculated using the lumped modified Xinanjiang hydrologic model and distributed SWAT model based on the water balance scheme, respectively. The relationship between actual daily ET estimated from MODIS images and basin-scale ET calculated from the hydrologic model were in good agreement with acceptable correlation coefficient. The results suggested that the algorithm is applicable and operational for estimating and mapping basin-scale distributed daily actual ET over the study area. In order to use the algorithm proposed by this paper for water resource management and agricultural decision making, the algorithm should be validated using more data and be tested under different environment and different land use scenario conditions in future work.

Key words | daily actual evapotranspiration, Laohahe River basin, MODIS, SWAT, Xinanjiang model

INTRODUCTION

Evapotranspiration (ET) is an important variable for water and energy balances on the Earth's surface (Rivas & Caselles 2004; Sobrino *et al.* 2007). The knowledge of the distribution of ET is a key factor in hydrology and agriculture, ecology and in other environmental studies. The accurate estimation of basin-scale actual ET is a difficult problem in hydrologic models due to the complex nature of soil evaporation and vegetation transpiration (Zhao 2007). Many station-based observations of actual ET were conducted in large-scale field experiments by using various measurement instruments such as lysimeters, Bowen ratio system and eddy covariance tower (Hall *et al.* 1992; Wang & Mitsuta 1992). In general, eddy covariance is often considered as the most reliable and advanced method for measuring

land surface energy fluxes. However, it is commonly recognized that conventional techniques employing point measurements to estimate the components of energy balance are only of local scales and cannot be extended to large areas due to the spatial heterogeneity of land surface processes (Pelgrum & Bastiaanssen 1996; Su 2002). Satellite remote sensing provides an unprecedented global coverage of critical hydrologic data which are logistically and economically impossible to obtain through ground-based observation networks (Jiang & Islam 2001). Formal spatial models can be generated to derive a quantitative assessment of the spatial distribution of actual ET. Many principal parameters such as net radiation and vapor pressure deficit are vital to drive most actual ET estimating models. Remote

Xiuqin Fang (corresponding author)
School of Earth Sciences and Engineering,
Hohai University,
China
E-mail: kinkinfang@gmail.com

Xiuqin Fang
Liliang Ren
Qiongfang Li
Xiaofan Liu
Fei Yuan
State Key Laboratory of Hydrology – Water
Resources and Hydraulic Engineering,
Hohai University,
Nanjing 210098,
China

Dengzhong Zhao
Spatial Information Technology Application
Department,
Changjiang River Scientific Research Institute,
Wuhan 430010,
China

Qian Zhu
Institute of Environment Sciences,
University of Quebec,
Montreal, H3C 3P8,
Canada

sensing and GIS-based modeling techniques make it possible and easier to derive these important parameters for actual ET mapping at basin or regional scale.

The objective of this study was to model the spatial distribution of actual ET over the Laohahe River basin, northeastern China using remotely sensed MODIS data and to evaluate the model performance. A lumped hydrologic model and a spatially distributed hydrologic model were separately utilized in this basin and actual ET calculated from a water balance equation using the hydrologic models was used to evaluate the performance of the ET estimation model from MODIS images.

The residual method is a commonly used scheme to calculate surface latent heat flux based on the surface energy balance:

$$\lambda E + H = R_n - G \quad (1)$$

where λE is the latent heat flux, H is the sensible heat flux, R_n is the net radiation (including long-wave and short-wave), and G is the soil heat flux. Obtaining spatial information of net radiation and soil heat flux is possible from satellite remote sensing images and derive information from them. But significant uncertainty exists in the estimation of sensible heat flux using remotely sensed data, because the aerodynamic resistance and surface roughness length are difficult to estimate accurately (Stewart *et al.* 1994; Chehbouni *et al.* 1996). Therefore, direct acquisition of sensible heat flux H from satellite observation was avoided in many studies on ET (Zhao 2007). The ratio of latent heat flux and available radiant energy was introduced to estimate ET from remote sensing images (Priestley & Taylor 1972; Jiang & Islam 2001; Wang *et al.* 2006, 2007; Venturini *et al.* 2008).

Parlange *et al.* (1995) provided a general form of various formulations describing ET:

$$\lambda E = \psi \left[A \frac{\Delta}{\Delta + \gamma} (R_n - G) + B \frac{\gamma}{\Delta + \gamma} f(u) (e_a^* - e_a) \right] \quad (2)$$

where e_a is the air vapor pressure at a reference height (often 2 m); e_a^* is the air saturation vapor pressure; Δ is the gradient of the saturated vapor pressure to the air temperature; ($\Delta = de_a^*/dT$), and γ is the psychrometric constant. The $f(u)$

term represents some function of the wind velocity; A and B are model-dependent parameters; and ψ is generally taken to be unity.

Equation (2) gives daily estimates of latent heat flux with high reliability when applied locally, but has been less successful when applied over large areas (Parlange *et al.* 1995). One of the major stumbling blocks is that we are unable to obtain effective regional values for the free parameters in these equations (Jiang & Islam 2001).

Priestley & Taylor (1972) simplified Equation (2) to

$$\lambda E = \alpha \left[(R_n - G) \frac{\Delta}{\Delta + \gamma} \right] \quad (3)$$

where $\alpha = 1.26$ is the Priestley–Taylor parameter. Equation (3) can form the basis for estimating evaporation over large areas using remote sensing observations. However, it is only applicable for water bodies and wet vegetation surfaces because it is suggested by a series of papers that the Priestley–Taylor expression with $\alpha = 1.26$ is a more accurate representation of evaporation under equilibrium wet surface conditions.

Based on the above study, Jiang & Islam (2001) adapted Equation (2) to

$$\lambda E = \varphi \left[(R_n - G) \frac{\Delta}{\Delta + \gamma} \right] \quad (4)$$

where φ is a modified form of the parameter α ranging from 0 to 1.26. Equation (4) can be treated as an extension of the Priestley–Taylor equation since the parameter φ uses a range of values, versus a single value of the Priestley–Taylor parameter α . More importantly, the Priestley–Taylor evaporation approach is primarily applicable for wet conditions, while the use of contextual information allows the application of Equation (4) over large heterogeneous areas (Jiang & Islam 2001).

It has been found that the modified Priestley–Taylor parameter φ can be estimated from the trapezoid feature space of Normalized Difference Vegetation Index (NDVI) and land surface temperature (Jiang & Islam 2001; Wan *et al.* 2004; Wang *et al.* 2006).

In this paper, an algorithm based on Equation (4) was applied to Moderate Resolution Imaging Spectroradiometer

(MODIS) data to estimate the spatial distribution of the daily ET over the Laohahe River basin, northeastern China. Because the direct measurement of observed actual ET is missing, we use actual ET calculated from water balance equation to evaluate the performance of ET estimation from MODIS images. The modified Xinanjiang hydrologic model (denoted XAJ model) and Soil and Water Assessment Tool (SWAT) model were used to calculate actual ET for the validation of the basin-scale actual evapotranspiration estimation algorithm from different aspects.

METHODS

Study area and data

The Laohahe River basin, with a total drainage area of 18,599 km², is controlled by the Xinglongpo hydrologic station (42°19' N, 119°26' E). It is a tributary of the West Liaohe River and situated in northeast China between 41°–43°18' N and 117°–120°30' E (Figure 1). It covers areas of Hebei Province, Liaoning Province and the Inner Mongolia Autonomous Region. Topographically, the Laohahe River basin shows well-pronounced variations, with elevation ranging from about 400 m at the channel outlet to around 2,000 m at the mountain ridges in the area (Figure 1).

The MODIS products were downloaded from the Level 1 and Atmosphere Archive and Distribution System (LAADS) (<http://ladsweb.nascom.nasa.gov/>) provided by National Aeronautics and Space Administration (NASA),

USA. A total of 22 MODIS images acquired under clear-sky conditions over the basin were used. The image acquisition period ranged from June to September 2000, covering the growing season.

Daily maximum and minimum air temperature data, collected from standard meteorological stations shown in Figure 1, were utilized to produce instantaneous air temperature on the days when MODIS images were acquired. Furthermore, 30" digital elevation model (DEM) data from Shuttle Radar Topography Mission (SRTM) were used in this study to make a watershed delineation and to calculate relative parameters for ET estimation.

Daily precipitation and pan evaporation data at precipitation gauges and daily stream flow data from 1999 to 2006 at hydrologic observation stations within the Laohahe River basin were collected for calibration and verification of model parameters.

Estimation of actual ET from MODIS images

The modified Priestley–Taylor parameter, ϕ

The modified Priestley–Taylor parameter, ϕ of each pixel of the MODIS images was calculated as follows (Jiang & Islam 2002; Wang et al. 2006):

$$\phi_i = \frac{LST_{\max} - LST_i}{LST_{\max} - LST_{\min}} (\phi_{\max} - \phi_{\min}) + \phi_{\min} \quad (5)$$

where LST_{\max} , LST_{\min} and LST_i are, respectively, the maximum, minimum and the estimated pixel land surface

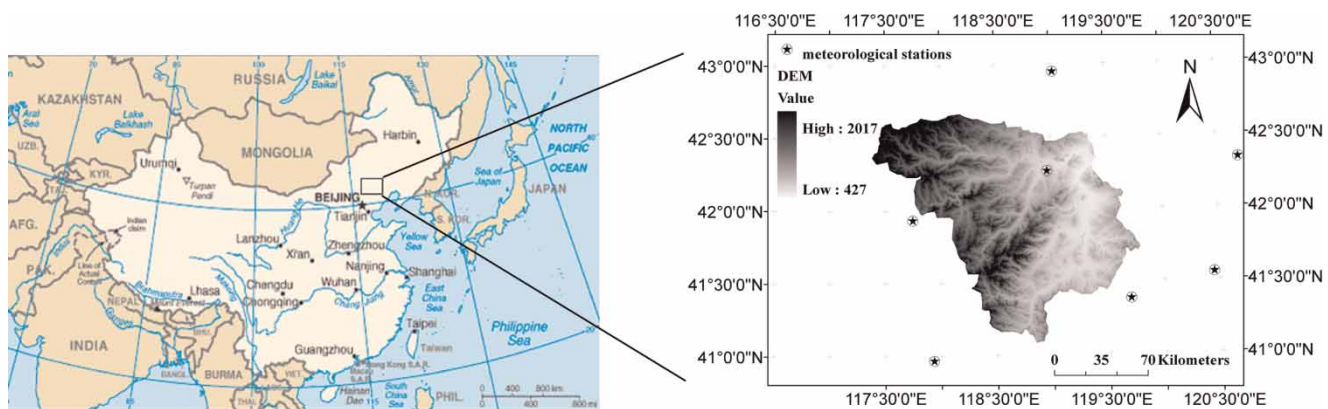


Figure 1 | Location and topography of the Laohahe River basin and the location of nearby meteorological stations.

temperature value in the image; $\varphi_{\max} = 1.26$, $\varphi_{\min} = 0$. In this method, the maximum value of φ ($=1.26$) corresponds to pixels with maximum ET under equilibrium surface moisture conditions, while a value of 0 for φ corresponds to pixels with no ET. The applicable split-window algorithm for retrieving land surface temperature from MODIS data was used (Mao *et al.* 2005).

Parameters Δ and γ

Richards (1971) suggested a simple algorithm to calculate Δ :

$$\Delta = \frac{373.15e^*}{T_a^2} (13.3185 - 3.952T_r - 1.9335T_r^2 - 0.5196T_r^3) \quad (6)$$

$$e^* = P_0 \exp(13.3185T_r - 1.976T_r^2 - 0.6445T_r^3 - 0.1299T_r^4) \quad (7)$$

$$T_r = 1 - 373.15/T_a \quad (8)$$

where T_a is instantaneous air temperature (K), which was calculated from daily maximum and minimum air temperature (Parton & Jogan 1981).

The psychrometric constant γ was calculated according to the research of FAO (Allen *et al.* 1998):

$$\gamma = 0.665 \times 10^{-5} P \quad (9)$$

$$P = 101.3 \left(\frac{293 - 0.0065z}{293} \right)^{5.26} \quad (10)$$

where P is atmospheric pressure (kPa), and z is elevation above sea level (m).

Net radiation, R_n

Net radiation R_n is calculated as

$$R_n = R_s(1 - \alpha) + R_{l\downarrow} - R_{l\uparrow} \quad (11)$$

where R_s is the incoming short-wave solar radiation (W m^{-2}); α is the surface albedo; $R_{l\downarrow}$ is the long-wave

downward radiation (W m^{-2}) from the atmosphere; and $R_{l\uparrow}$ is the long-wave upward radiation from land surface (W m^{-2}).

The parameter R_s is calculated as

$$R_s = K_0 \cdot dr \cdot \tau_{sw} \cos \theta \quad (12)$$

where K_0 is the solar constant at the top of the atmosphere ($=1,370 \text{ W m}^{-2}$); dr is the Sun–Earth distance calculated from the day of year; τ_{sw} is the atmospheric clear-sky short-wave transmission factor; and θ is the solar zenith angle. The factor τ_{sw} is obtained by (Tasumi *et al.* 2000)

$$\tau_{sw} = 0.75 + 2 \times 10^{-5} Z \quad (13)$$

where Z is pixel elevation obtained from DEM data.

The parameter α is calculated from linear combination bands following Liang's model (Liang 2001):

$$\alpha = 0.16R(1) + 0.29R(2) + 0.24R(3) + 0.116R(4) + 0.112R(5) + 0.081R(7) - 0.0015 \quad (14)$$

where $R(i)$ is the i th band's reflectance of MODIS images.

Given a certain atmospheric condition, the atmospheric long-wave downward radiation ($R_{l\downarrow}$) is expected to be homogeneous over a large synoptic area (Jiang & Islam 2001). Thus the measurements of $R_{l\downarrow}$ from the Chifeng ground station within the study area were applied to the whole study region.

The parameter $R_{l\uparrow}$ is calculated as

$$R_{l\uparrow} = \varepsilon_s \sigma T_s^4 \quad (15)$$

where ε_s is the land surface emissivity; σ is the Stefan–Boltzmann constant ($5.67 \times 10^{-8} \text{ W m}^{-2} \text{ K}^{-4}$); and T_s is the land surface temperature (K). According to Sobrino *et al.* (2001), ε_s can be calculated from an empirical relationship with NDVI:

$$\varepsilon_s = \begin{cases} 1.009 + 0.047 \ln(\text{NDVI}1) & \text{when NDVI} > 0 \\ 0, & \text{otherwise} \end{cases} \quad (16)$$

and NDVI is obtained using the reflectance of the second

and first bands ($R(2)$ and $R(1)$) of MODIS images:

$$\text{NDVI} = \frac{R(2) - R(1)}{R(2) + R(1)} \quad (17)$$

Soil heat flux, G

Although soil heat flux often changes with time, the magnitude is small compared to net radiation over dense vegetation. Soil heat flux generally can be estimated according to relationships between the above parameters R_n , T_s , α and NDVI (Bastiaanssen *et al.* 1998):

$$G = (T_s - 273.15)[0.0036 + 0.0077\alpha](1 - 0.978\text{NDVI}^4)R_n \quad (18)$$

where T_s is land surface temperature (K).

Daily actual ET

The ET estimated from MODIS data was instantaneous for the time of the satellite sensor overpass. According to the model by Jackson *et al.* (1983), the instantaneous ET (E_i) can be converted to daily actual total ET under the assumption that the diurnal change of ET is similar to that of solar irradiance on a clear day. The method is

$$E_d = E_i \left[\frac{2N}{\pi \sin(\pi \cdot t/N)} \right] \quad (19)$$

$$N = 0.945[a + b \sin^2(\pi(D + 10)/365)] \quad (20)$$

$$a = 12.0 - 5.96 \times 10^{-2}L - 2.02 \times 10^{-4}L^2 + 8.25 \times 10^{-4}L^3 - 3.15 \times 10^{-7}L^4 \quad (21)$$

$$b = 0.123L - 3.10 \times 10^{-4}L^2 + 8.00 \times 10^{-7}L^3 + 4.99 \times 10^{-7}L^4 \quad (22)$$

where E_d is the daily ET, t is the time (beginning at sunrise) when a MODIS image is acquired, N is the time period between sunrise and sunset in units of t , D is the day of year, and L is the pixel's latitude.

Hydrologic models

XAJ model

The XAJ model is a conceptual basin-scale hydrologic model. It is widely applied in China because of model feasibility and parameter transferability. The core of the XAJ model is the storage capacity distribution curves of tension water and free water, which describe their spatial heterogeneity within a basin (Zhao 1992). The ET component is estimated with a model using three soil layers. A modified XAJ model called hybrid runoff model (Hu 1993) was used in this paper. Numerous field studies show that runoff within a basin is mainly generated by two mechanisms: infiltration excess (Horton) runoff and saturation excess (Dunne) runoff. The hybrid runoff model combines the two runoff mechanisms by means of the combination of spatial distribution curve of soil tension water storage capacity and that of infiltration capacity.

The combination of the two runoff mechanisms is the way by which daily runoff simulation and flood forecasting were done in the Laohahe River basin (Liu *et al.* 2009). The hybrid runoff model was successfully used in the Laohahe catchment for daily runoff simulation and flood forecasting (Ren *et al.* 2006; Yuan & Ren 2008). The detailed description of the mechanisms and application of the modified XAJ model used in this study was showed by Liu *et al.* (2009).

Daily actual ET calculated from XAJ model was lumped which meant only an average value was used each day over the study area.

SWAT model

SWAT is a distributed hydrologic model providing spatial coverage of the integral hydrologic cycle including fluxes through atmosphere, plants, unsaturated zone, groundwater, and surface water (Immerzeel & Droogers 2008). The model is comprehensively described in the literature (Arnold *et al.* 1998; Srinivasan *et al.* 1998; Arnold & Fohrer 2005). Conceptually SWAT subdivides the catchment into subbasins and a river network based on DEM data. Based on unique combinations of soil and land use, the sub-basins were further detailed into hydrologic response units (HRUs), which

were the fundamental units of calculation. A total of 33 sub-basins and 202 HRUs were delineated in the Laohahe River catchment (Figure 2).

There are nine hydrologic monitoring stations including the watershed outlet Xinglongpo station in the Laohahe River catchment (Figure 2). Calibration and validation of the SWAT output was performed by comparing predicted flow and with corresponding in-stream measurements at the nine hydrologic stations from 1999 to 2006. The calculation was carried out from upstream gauges to downstream gauges, beginning with the Dianzi station. The next downstream station at Xiaochengzi was completed to the same level of detail. The rest was processed analogically. Finally, the Xinglongpo site was calibrated most intensively. After average annual discharge rates were acceptable with the relative error between model-simulated and measured average annual discharges below 15%,

SWAT-predicted monthly and daily hydrographs at the nine sites were compared to observed data for further calibration. The time period for calibration was 1999–2003 and the remaining data from 2004–2006 to be used for model validation. The performance of the model is measured using the Nash–Sutcliffe efficiency (NS, Equation (23)) and *r*-squared (R^2 , Equation (24)):

$$NS = 1 - \frac{\sum_{i=1}^N (Q_{obs_i} - Q_{sim_i})^2}{\sum_{i=1}^N (Q_{obs_i} - \overline{Q_{obs}})^2} \quad (23)$$

$$R^2 = \left[\frac{\sum_{i=1}^N (Q_{obs_i} - \overline{Q_{obs}})(Q_{sim_i} - \overline{Q_{sim}})}{\sum_{i=1}^N (Q_{obs_i} - \overline{Q_{obs}})^2 \sum_{i=1}^N (Q_{sim_i} - \overline{Q_{sim}})^2} \right]^2 \quad (24)$$

where Q_{obs_i} is observed streamflow (m^3/s) at time step i , Q_{sim_i} is the simulated streamflow (m^3/s) at time step i ,

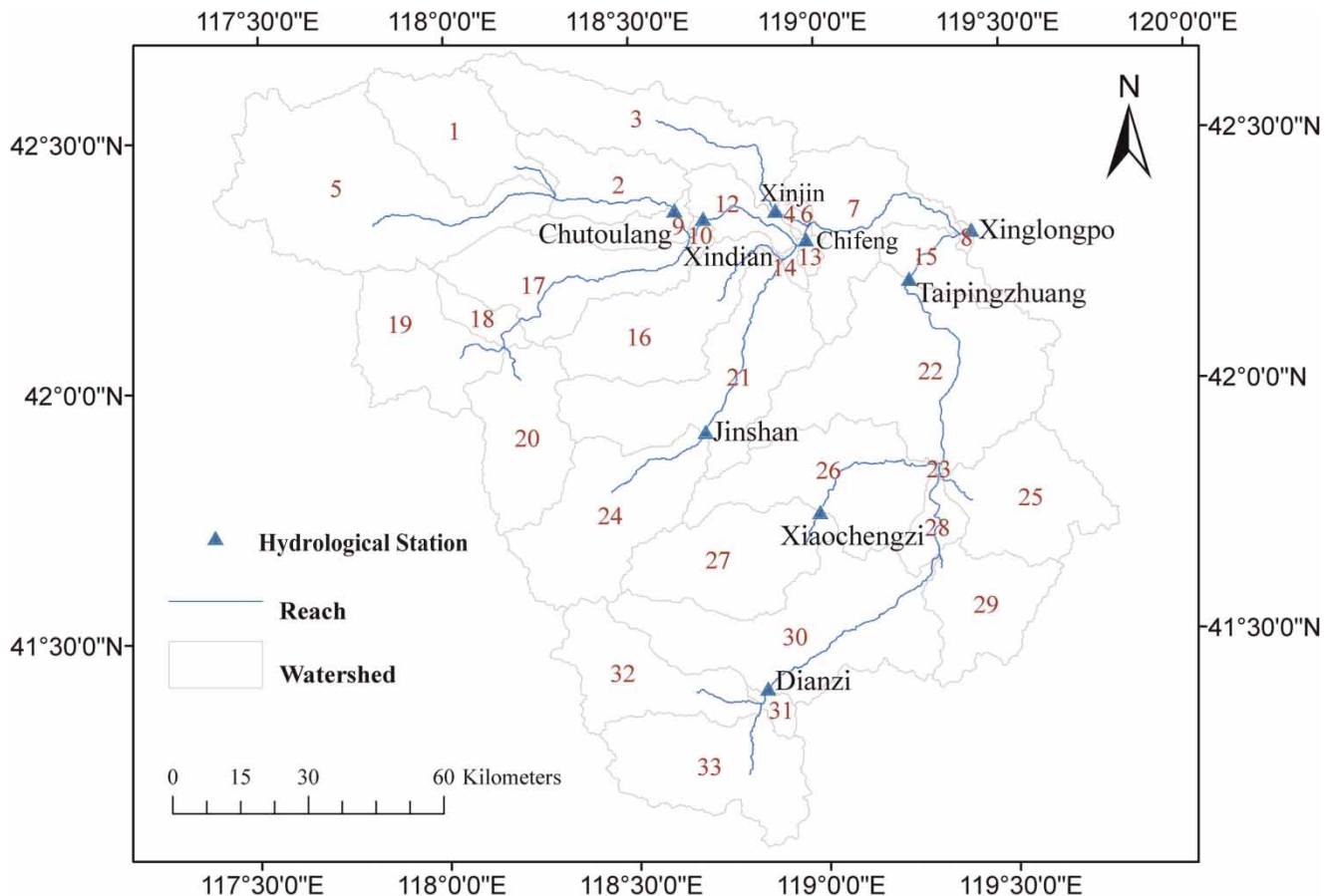


Figure 2 | Sub-basins and hydrologic stations of the Laohahe River basin.

$\overline{Q_{sim}}$ and $\overline{Q_{sim}}$ are the mean of the observed and simulated values respectively (m^3/s), and N is the number of data points. The Nash–Sutcliffe efficiency is a statistical measure that is more stringent than R^2 because it compares two variables assuming a 1:1 relationship rather than measuring deviation from the best fit line as with R^2 measures. Nash–Sutcliffe efficiency values greater than or equal to 0.50 are thus considered adequate for SWAT model applications (Santhi et al. 2001). Estimated ET could not be directly validated because of the lack of measured ET. So it was indirectly validated by means of streamflow which could be validated using R^2 and Nash–Sutcliffe efficiency. In this study, as for year 2000, monthly statistics showed values of 0.76 and 0.64 for R^2 and Nash–Sutcliffe efficiency, respectively.

Daily actual ET from SWAT model was relatively distributed as each sub-basin had an ET value each day which was one of the hydrologic outputs of SWAT. So we collected 33 ET values from the 33 sub-basins each day over the study area. And we also collected an average ET value of the whole catchment each day which is the area-weighted average of all the 33 ET values from the 33 sub-basins.

Statistical test run to compare MODIS and model estimates of ET

In this study, ET estimated from MODIS images was pixel-scale, while ET calculated from XAJ and SWAT hydrologic models was not. In order to statistically evaluate the ET estimation model from MODIS images using hydrologic model results, ET estimated MODIS images should be aggregated.

In order to be compared with ET calculated from the XAJ model, ET estimated from MODIS was aggregated as an arithmetical mean throughout the whole basin each day which spatially matched the XAJ outputs. To be compared with ET calculated from SWAT model, ET estimated from MODIS was aggregated as an arithmetical mean at each sub-basin each day which spatially matched the SWAT outputs. As for the latter comparison, we also computed an arithmetical mean of ET from MODIS images throughout the whole basin each day to compare it with the area-weighted average ET value of the whole catchment from SWAT model outputs.

RESULTS AND DISCUSSION

In this study we obtained spatial distributed mapping of daily ET for 22 clear-sky days between DOY 157 and 274 in the year 2000 from MODIS images over the Laohahe River basin, northeastern China. Hydrologic modeling based on the modified XAJ model and the SWAT model were carried out for the selected 22 days. To compare ET estimated from MODIS images with the ET predicted from the hydrologic model, spatially statistic analysis based on GIS techniques was utilized to extract averages of ET estimated from MODIS over the whole basin or sub-basins.

Figure 3 shows the relationship between actual daily ET estimated from MODIS images and calculated from the XAJ hydrologic model. The results of daily actual ET calculated from XAJ model were calculated over Taipingzhuang catchment (Liu et al. 2009), east of the Laohahe River Basin. The model gave 22 daily ET values in the selected 22 days over the whole catchment. It can be seen in Figure 3 that there was a good agreement between both ET, with R^2 and slope coefficient of 0.8153 and 1.0002, respectively.

Table 1 is a table of statistics of relationships between MODIS-estimated ET and SWAT-calculated ET for all 33 sub-basins used in the study. It can be seen that there were good agreements between both ET for almost all 33 sub-basins, with all R^2 values larger than 0.56 and half of them larger than 0.80. Moreover, average daily ET values of 22 days of the whole catchment and daily ET values of

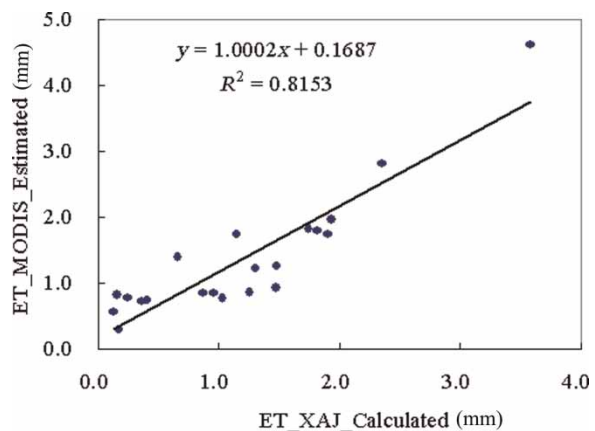


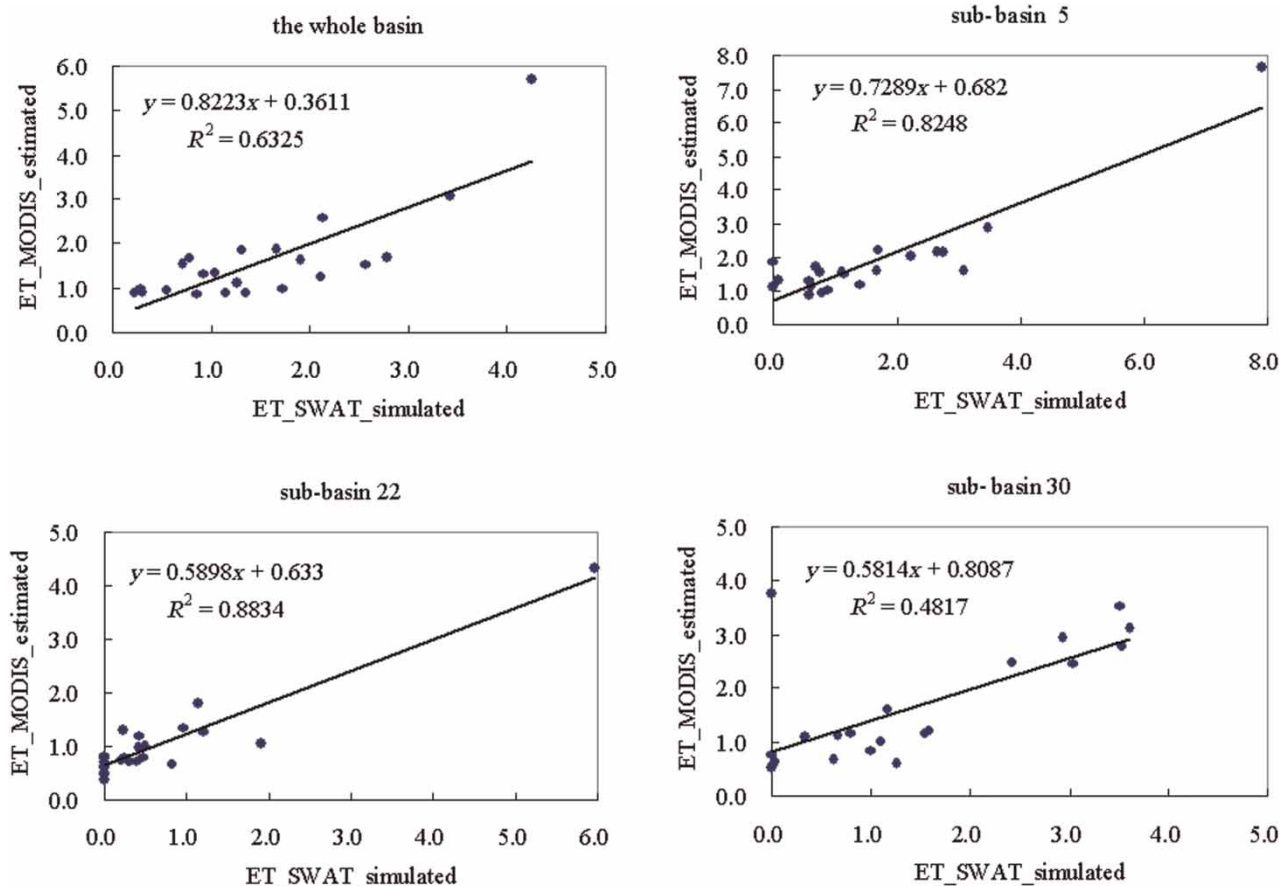
Figure 3 | Relationship between actual daily ET estimated from MODIS images and calculated from the XAJ model.

Table 1 | Statistics of relationship between ET estimated from MODIS images and ET calculated from the SWAT model for 33 sub-basins.

Sub-basin	R^2	Sub-basin	R^2	Sub-basin	R^2
1	0.6143	12	0.8348	23	0.8987
2	0.8103	13	0.7483	24	0.7622
3	0.6836	14	0.8113	25	0.8059
4	0.7857	15	0.7034	26	0.8147
5	0.8248	16	0.6258	27	0.7456
6	0.6946	17	0.6411	28	0.7424
7	0.7086	18	0.5981	29	0.7546
8	0.8636	19	0.7155	30	0.8817
9	0.8897	20	0.8501	31	0.7868
10	0.8405	21	0.8482	32	0.5687
11	0.8018	22	0.8834	33	0.9120

three representative sub-basins (sub-basins 5, 22 and 30) were selected to be shown in Figure 4. These representative sub-basins were selected based on the following considerations: (1) they are the three largest sub-basins in the study area; (2) sub-basin 5 lies in a semi-arid region, sub-basin 30 lies in a humid region, and sub-basin 22 lies in a semi-humid region; (3) sub-basin 5 and sub-basin 30 are upstream and sub-basin 22 is relatively downstream.

It can be seen from Figure 4 that there is good agreement between actual daily ET estimated from MODIS images and ET calculated from the SWAT hydrologic model. For the whole basin, there was a relatively good agreement between ET estimated from MODIS images and ET calculated from the SWAT model, with R^2 and slope coefficient of 0.6743 and 0.8715, respectively. Regarding the representative sub-basins, the relationship between both ETs showed better agreement with correlation

**Figure 4** | Relationship between actual daily ET estimated from MODIS images and ET calculated from the SWAT model.

coefficients of 0.8248, 0.8834, and 0.8817 for the three representative sub-basins (sub-basin 5, sub-basin 22 and sub-basin 30) respectively. The results mean that the ET estimation algorithm using MODIS data is applicable to the whole catchment and to the spatially different sub-basins ranging from semi-arid, to semi-humid and humid.

On the other hand, the results in Figure 4 also showed different characteristics of the relationship between ET estimated from MODIS images and calculated from the SWAT model corresponding to spatially different sub-basins. It can be seen that the ET of both the humid sub-basin 30 and semi-humid sub-basin 22 showed better agreement than that of semi-arid sub-basin 5. Comparing Figures 3 and 4, we can see that the agreement between ET calculated from the SWAT hydrologic model and ET estimated from the MODIS images over the whole catchment is worse than the agreement between ET calculated from XAJ and ET from MODIS images over the eastern humid and semi-humid Taipingzhuang catchment. These results should not be used to deduce a different applicability of the ET estimation algorithm from MODIS images in different regions, because better agreement between both ETs principally depended on better applicability of the hydrologic models in the humid and sub-humid areas than in the arid and sub-arid areas.

CONCLUSION

An algorithm was developed based on the surface energy balance equation and the modified Priestley–Taylor model for the estimation of the distributed daily actual ET using MODIS images. In this algorithm, a practical split-window algorithm for retrieving land surface temperature from MODIS data was applied. Parton's model for simulating diurnal changes of air temperature was used to obtain instantaneous near-surface air temperature at the satellite sensor passing. The trapezoid feature space of land surface temperature and NDVI was used to interpolate the modified Priestley–Taylor parameters for each pixel of the images, under the assumption that the diurnal change of ET is similar to the solar irradiance on a clear day to convert instantaneous ET into daily total ET for mapping surface energy flux and daily actual ET.

The algorithm was used to estimate actual daily ET from MODIS images during the growing seasons over the

Laohahe River basin, northeastern China. Regional daily ET computed by the lumped XAJ hydrologic model and distributed SWAT model based on the water balance scheme were used to validate the estimated ET values derived from remotely sensed data. Daily ET estimated from MODIS images and ET calculated from XAJ and SWAT hydrologic models based on the water balance scheme showed good agreement, which demonstrated that the method used for estimating ET with MODIS images based on the surface energy balance scheme and the modified Priestley–Taylor equation is applicable and operational for estimating and mapping daily actual ET over the study area.

ET values calculated from a hydrologic model can be indirectly calibrated based on the water balance scheme with measured discharge data. And ET values estimated from remotely sensed data is generally based on the surface energy balance scheme. ET estimation using remote sensing data can provide more detailed spatial resolution than the ET values calibrated from a hydrologic model. Actually speaking, none of the ET values from both approaches can be considered as 'actual' ET. However, it demonstrates the potential of the remote sensing data in the estimation of ET in a watershed. In future work, basin-scale actual ET can be computed using a new approach based on the combination of the water balance scheme and surface energy balance scheme.

In order to use the algorithm proposed by this paper for water resource management and agricultural decision making, the algorithm should be validated using more data and be tested under different environments and different land use scenario conditions in future work.

ACKNOWLEDGEMENTS

This research was supported financially by the National Key Basic Research Program of China under Project No. 2006CB400502 and the Fundamental Research Funds for the Central Universities. Also this research is the result of the 111 Project under Grant B08048, Ministry of Education and State Administration of Foreign Experts Affairs, P. R. China. It is a partial product of National High-Tech Research and Development Program under Grant 2008AA12Z202, the National Natural Science Foundation of China (Grant Nos. 50909033 and

40911130507) and Specialized Research Fund for the Doctoral Program of Higher Education from the Ministry of Education of China (Grant No. 20090094120010).

REFERENCES

- Allen, R. G., Pereira, L. S., Raes, D. & Smith, M. 1998 *Crop Evapotranspiration – Guidelines for Computing Crop Water Requirements*. FAO Irrigation and Drainage Paper 56. Food and Agriculture Organization of the United Nations, Rome.
- Arnold, J. G. & Fohrer, N. S. 2005 *WAT2000: current capabilities and research opportunities in applied watershed modeling*. *Hydrol. Process.* **19**, 563–572.
- Arnold, J. G., Srinivasan, P., Muttiah, R. S. & Williams, J. R. 1998 *Large area hydrologic modeling and assessment. Part I: Model development*. *J. Am. Water Resour. Ass.* **34**, 73–89.
- Bastiaanssen, W. G. M., Menenti, M., Feddes, R. A. & Holtslag, A. A. M. 1998 *A remote sensing surface energy balance algorithm for land (SEBAL). 1: Formulation*. *J. Hydrol.* **212–213**, 198–212.
- Chehbouni, A., Seen, D. L., Njoku, E. G. & Monteny, B. M. 1996 *Examination of the difference between radiative and aerodynamic surface temperature over sparsely vegetated surfaces*. *Remote Sens. Environ.* **58**, 177–186.
- Hall, F. G., Huemmrich, K. F., Goetz, S. J., Sellers, P. J. & Nickeson, J. E. 1992 *Satellite remote sensing of surface energy balance: success, failures, and unresolved issues in FIFE*. *J. Geophys. Res.* **97** (D17), 19,061–19,089.
- Hu, C. Q. 1993 *Computational method of runoff generation in semi-humid and semi-arid regions*. In *Symposium on Hydrological Information and Forecasting*. (In Chinese.) China Water Power Press, Beijing, pp. 57–62.
- Immerzeel, W. W. & Droogers, P. 2008 *Calibration of a distributed hydrological model based on satellite evapotranspiration*. *J. Hydrol.* **349**, 411–424.
- Jackson, R. D., Hatfield, J. L., Reginato, R. J., Idso, S. B. & Pinter Jr., P. J. 1985 *Estimation of daily evapotranspiration from one time-of-day measurements*. *Agr. Water Manage.* **7** (1–3), 351–362.
- Jiang, L. & Islam, S. 2001 *Estimation of surface evaporation map over southern Great Plains using remote sensing data*. *Water Resour. Res.* **37** (2), 329–340.
- Liang, S. 2001 *Narrowband to broadband conversion of land surface albedo I. Algorithms*. *Remote Sens. Environ.* **76** (2), 213–238.
- Liu, X., Ren, L., Yuan, F., Singh, V. P., Fang, X., Yu, Z. & Zhang, W. 2009 *Quantifying the effect of land use and land cover changes on green water and blue water in northern part of China*. *Hydrol. Earth Syst. Sci.* **13**, 735–747.
- Mao, K., Qin, Z., Shi, J. & Gong, P. 2005 *A practical split-window algorithm for retrieving land-surface temperature from MODIS data*. *Int. J. Remote Sens.* **26** (15), 3181–3204.
- Parlange, M. B., Eichinger, W. E. & Albertson, J. D. 1995 *Regional scale evaporation and the atmospheric boundary layer*. *Rev. Geophys.* **33** (1), 99–124.
- Parton, W. J. & Jogan, J. A. 1981 *A model for diurnal variation in soil and air temperature*. *Agric. Met.* **23**, 205–216.
- Pelgrum, H. & Bastiaanssen, W. 1996 *An intercomparison of techniques to determine the area-averaged latent heat flux from individual in situ observations: a remote sensing approach using the European field experiment in a desertification-threatened area data*. *Water Resour. Res.* **32**, 2775–2786.
- Priestley, C. H. B. & Taylor, R. J. 1972 *On the assessment of surface heat flux and evaporation using large-scale parameters*. *Mon. Weather Rev.* **100**, 81–92.
- Ren, L., Huang, Q., Yuan, F., Wang, J., Xu, J., Yu, Z. & Liu, X. 2006 *Evaluation of the Xinanjiang model structure by observed discharge and gauged soil moisture data in the HUBEX/GAME Project*. In IAHS-AISH Publication no. 303, pp. 153–163.
- Richards, J. M. 1971 *Simple expression for the saturation vapor pressure of water in the range -50° to 140°* . *Br. J. Appl. Phys.* **4**, 115–118.
- Rivas, R. & Caselles, V. 2004 *A simplified equation to estimate spatial reference evaporation from remote sensing-based surface temperature and local meteorological data*. *Remote Sens. Environ.* **93**, 68–76.
- Santhi, S., Arnold, J. G., Williams, J. R., Dugas, W. A., Srinivasan, R. & Hauck, L. M. 2001 *Validation of SWAT model on a large river basin with point and nonpoint sources*. *J. Am. Water Resour. Ass.* **37**, 1169–1188.
- Sobrino, J. A., Gómez, M., Jiménez-Muñoz, J. C. & Oliso, A. 2007 *Application of a simple algorithm to estimate daily evapotranspiration from NOAA-AVHRR images for the Iberian Peninsula*. *Remote Sens. Environ.* **110**, 139–148.
- Sobrino, J. A., Raissouni, N. & Li, Z. L. 2001 *A comparative study of land surface emissivity retrieval from NOAA data*. *Remote Sens. Environ.* **75**, 256–266.
- Srinivasan, R., Ramanarayanan, T. S., Arnold, J. G. & Bednarz, S. T. 1998 *Large area hydrologic modeling and assessment part II: model application*. *J. Am. Water Resour. Ass.* **34**, 91–101.
- Stewart, J. B., Kustas, W. P., Humes, K. S., Nichols, W. D., Moran, M. S. & Bruin, H. A. R. D. 1994 *Sensible heat flux – Radiometric surface temperature relationship for eight semiarid areas*. *J. Appl. Meteorol.* **33**, 1110–1117.
- Su, Z. 2002 *The surface energy balance system (SEBS) for estimation of turbulent heat fluxes*. *Hydrol. Earth Syst. Sci.* **6**, 85–100.
- Tasumi, M., Bastiaanssen, W. & Allen, R. G. 2000 *Application of the SEBAL methodology for estimating consumptive use of water and stream flow depletion in the Bear River Basin of Idaho through Remote Sensing*. Report submitted to Earth Observation System Data and Information System Project, Raytheon Systems Company and the University of Idaho.

- Venturini, V., Islam, S. & Rodriguez, L. 2008 Estimation of evaporative fraction and evapotranspiration from MODIS products using a complementary based model. *Remote Sens. Environ.* **112**, 132–141.
- Wan, Z., Wang, P. & Li, X. 2004 Using MODIS land surface temperature and normalized difference vegetation index products for monitoring drought in the Southern Great Plains, USA. *Int. J. Remote Sens.* **25** (1), 61–72.
- Wang, J. M. & Mitsuta, Y. 1992 An observational study of turbulent structure and transfer characteristics in Heihe Oasis. *J. Meteorol. Soc. Japan* **70** (6), 1147–1154.
- Wang, K., Li, Z. & Cribb, M. 2006 Estimation of evaporative fraction from a combination of day and night land surface temperatures and NDVI: a new method to determine the Priestley–Taylor parameter. *Remote Sens. Environ.* **102** (3–4), 293–305.
- Wang, K., Wang, P., Li, Z., Cribb, M. & Sparrow, M. 2007 A simple method to estimate actual evapotranspiration from a combination of net radiation, vegetation index, and temperature. *J. Geophys. Res.* **112** (D15107).
- Yuan, F. & Ren, L. 2008 Evaluating the influence of land-cover change on catchment hydrology through the modified Xinanjiang model. In *Hydrological Sciences for Managing Water Resources in the Asian Developing World*. IAHS–AISH Publication no. 319, pp. 167–174.
- Zhao, D. 2007 Assimilation of remotely sensed evapotranspiration with the ESSI distributed hydrological model over the Jinghe River Basin, China. PhD Thesis, School of Geographic and Oceanographic Sciences, Nanjing University, Nanjing.
- Zhao, R. J. 1992 The Xinanjiang model applied in China. *J. Hydrol.* **135** (3), 371–381.

First received 8 October 2009; accepted in revised form 22 April 2010. Available online December 2011